

Quantum Pumping and Quantized Magnetoresistance in a Hall Bar

M. Blaauboer

Department of NanoScience, Delft University of Technology, Lorentzweg 1, 2628 CJ Delft, The Netherlands

(Dated: November 20, 2018)

We show how a dc current can be generated in a Hall bar without applying a bias voltage. The Hall resistance R_H that corresponds to this pumped current is quantized, just as in the usual integer quantum Hall effect (IQHE). In contrast with the IQHE, however, the longitudinal resistance R_{xx} does not vanish on the plateaus, but equals the Hall resistance. We propose an experimental geometry to measure the pumped current and verify the predicted behavior of R_H and R_{xx} .

PACS numbers: 72.10.Bg, 73.43.Cd, 73.23.-b

I. INTRODUCTION

The phenomenon of quantum pumping has received a lot of attention in recent years^{1,2,3}. It involves the generation of a dc current of electrons through ac modulation of their environment, e.g. the potential landscape or a magnetic field. This requires that at least two independent system parameters are varied in a periodic manner, and with a phase difference ϕ between them⁴. If the resulting current depends on quantum-mechanical interference in the system, this process is named “quantum pumping”, in contrast with “classical” pumping in which particles are pumped sequentially⁵. So far, quantum pumping has mainly been studied in the context of charge⁶ and spin⁷ pumping in quantum dots, small islands embedded in a semiconductor material⁸. In this work, we focus on a new pumping geometry: a Hall bar in the integer quantum Hall regime, see Fig. 1. We recently proposed how quantum pumping in such a system may be used to control and measure the local polarization of the nuclei present in the system⁹. Here we study in more detail the pumped current itself and investigate the corresponding perpendicular (Hall) and parallel resistance. Using a Floquet scattering approach, we show that in the regime of weak pumping and low temperatures the pumped current exhibits typical pumping characteristics such as linear dependence on the pumping frequency ω , quadratic dependence on the pumping strength and sinusoidal dependence on the phase difference ϕ . For stronger pumping, numerical analysis shows that the latter disappears, although the periodicity in ϕ remains, and that the current becomes more sharply peaked. We then calculate the Hall resistance and find that it exhibits steplike behavior as a function of the applied magnetic field. We also calculate the longitudinal resistance R_{xx} which turns out to be identical to R_H . This can be explained in terms of the intrinsic scattering nature of quantum pumping.

II. QUANTUM PUMPING

Let us start by considering the geometry schematically depicted in Fig. 1. It consists of a Hall bar placed in a sufficiently strong magnetic field, so that electrons

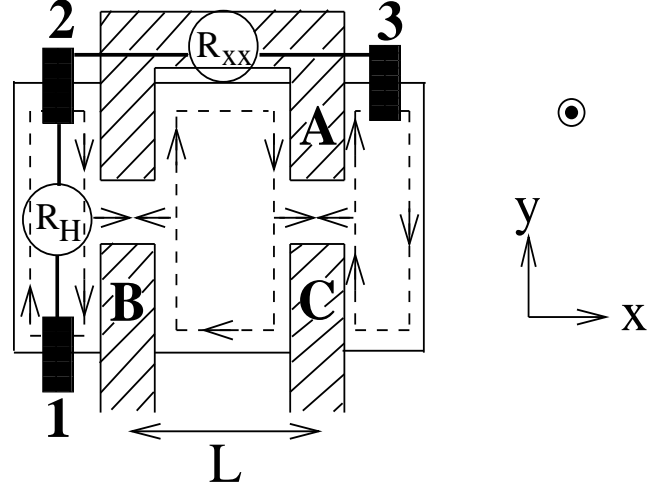


FIG. 1: Schematic picture of a Hall bar at bulk filling factor $\nu = 1$ with a magnetic field applied perpendicular to the plane of the paper. Current (dashed lines) flows along the edges of the sample and is scattered at the two quantum point contacts AB and AC (shaded). See the text for further explanation.

travel in one-dimensional channels along the boundaries of the sample¹⁰. These so-called edge channels correspond to quantized energy levels, the Landau levels, which are macroscopically degenerate, capable of holding many electrons. The number of filled Landau levels is characterized by the filling factor $\nu \equiv n_e h / (eB)$, where n_e denotes the electron density and B the applied magnetic field. The Hall bar in Fig. 1 contains three contacts 1-3 which can be used to measure the voltage drops perpendicular and parallel to the direction of the current. It also contains three voltage gates A, B, and C which, combined as the split-gate pairs AB and AC, form two quantum point contacts (QPCs). By applying time-varying voltages with a phase difference ϕ to gates B and C, these gates may serve as pumping parameters. To begin with, we concentrate on the regime of $\nu = 1$ and assume the QPCs transmit at most one edge channel. Part of the electrons in the edge channel are then reflected at, and part of them transmitted through each QPC, as depicted in Fig. 1. Since transport is effectively one-dimensional, we model the QPCs by δ -function potential

barriers¹¹ $V_{AB}(x, t) = [\bar{V}_{AB} + 2\delta V_{AB} \cos(\omega t)] \delta(x + \frac{L}{2})$ and $V_{AC}(x, t) = [\bar{V}_{AC} + 2\delta V_{AC} \cos(\omega t + \phi)] \delta(x - \frac{L}{2})$. The time-dependent parts represent the pumping voltages, applied to gates B and C, with ω the pumping frequency and ϕ a phase difference¹². In order to calculate the pumped current, we use a Floquet scattering approach^{13,14}. This approach describes the scattering of electrons at an oscillating barrier in terms of the gain or loss of energy quanta $\hbar\omega$. If an incoming electron has energy E , the outgoing state after interaction with the barrier is characterized by energies $E_n \equiv E + n\hbar\omega$, with $n = \dots, -2, -1, 0, 1, 2, \dots$. The Floquet theorem states that this is the full set of energies for outgoing particles¹³ and the scattering process is represented by the Floquet scattering matrix S_{FL} . The matrix elements $t_{\alpha\beta}(E_n, E)$ of S_{FL} represent the scattering amplitude of an electron that arrives at the barrier from contact β with energy E and leaves to contact α with energy E_n . The pumped current into contact α , with in our case $\alpha = 1, 2$ or 3 , is then given by¹⁴

$$I_\alpha = \frac{e}{h} \int dE f(E) \sum_{\beta} \sum_{E_n > 0} (|t_{\alpha\beta}(E_n, E)|^2 - |t_{\beta\alpha}(E_n, E)|^2). \quad (1)$$

Here $f(E) = (1 + \exp[(E - \mu)/(k_B T)])^{-1}$ denotes the Fermi distribution, with μ the chemical potential in the leads, and we have assumed that incoming electrons in different leads are described by the same Fermi function. This is in agreement with our pumping set-up, where no bias voltage is applied and all contacts are held at the same chemical potential μ . Under these circumstances, current flows out of and into each contact 1, 2 and 3, as sketched in Fig. 1: all electrons emerging from contact 1 will flow into contact 2, the ones emerging from contact 2 are scattered at the QPC's and go to contact 1 or 3, and electrons coming out of contact 3 are either scattered back into 3 or end up in contact 1. We are interested in the net current flow I_α into each contact $\alpha = 1, 2, 3$. It is easy to see that $I_2 = 0$, since the amount of incoming and outgoing electrons at contact 2 is the same. So, in order to calculate the pumped current, it is sufficient to consider a two-terminal geometry, omitting contact 2, and

$$I_1 = -I_3 = \frac{e}{h} \int dE f(E) \sum_{E_n > 0} (|t_{13}(E_n, E)|^2 - |t_{31}(E_n, E)|^2). \quad (2)$$

Now it remains to calculate the scattering amplitudes. This is done by matching the appropriate wavefunctions at the two δ -function barriers, as was recently done for one-dimensional mesoscopic quantum pumps^{14,15}. The wavefunction describing electron transport along the edge channels is given by the solution of the Schrödinger equation $i\hbar \frac{\partial}{\partial t} \psi(x, y, t) = \mathcal{H} \psi(x, y, t)$ with

$$\mathcal{H} = \frac{1}{2m^*} (i\hbar \vec{\nabla} + e\vec{A})^2 + V(y). \quad (3)$$

Here m^* denotes the effective mass, \vec{A} the vector potential and $V(y)$ the transverse confining potential¹⁶. We now take the Landau gauge $A_x = -By$ and assume that the transverse confining potential can be described by a harmonic potential, $V(y) = \frac{1}{2}m^*\omega_0^2 y^2$. The latter gives a good description of transport at the edges if $V(y)$ is constant on the scale of the magnetic length $l_m \equiv \left(\frac{\hbar}{m^* \sqrt{\omega_0^2 + \omega_c^2}} \right)^{1/2}$, with $\omega_c \equiv |e|B/m^*$ the cyclotron frequency^{17,18}. The solution of the Schrödinger equation with the Hamiltonian (3) is then given by¹⁹

$$\psi_\lambda(x, y, t) = C_\lambda \chi_\lambda(y) e^{i(kx - \frac{E_\lambda}{\hbar} t)}, \quad (4)$$

$$\chi_\lambda(y) = e^{\frac{1}{2l_m}(y + \frac{\omega_c^2}{\omega_0^2 + \omega_c^2} y_k)^2} \times \left(\frac{\partial}{\partial y} \right)^\lambda e^{-\frac{1}{2l_m}(y + \frac{\omega_c^2}{\omega_0^2 + \omega_c^2} y_k)^2} \quad (5)$$

$$E_\lambda = \left(\lambda + \frac{1}{2} \right) \hbar \sqrt{\omega_0^2 + \omega_c^2} + \frac{1}{2} m^* \frac{\omega_0^2 \omega_c^2}{\omega_0^2 + \omega_c^2} y_k^2, \quad \text{for } \lambda = 0, 1, 2, \dots \quad (6)$$

Here C_λ denotes a normalization constant, $y_k \equiv \hbar k / eB$, and E_λ the Landau levels measured from the lowest band imposed by the confinement in the z -direction. When the two time-dependent δ -function potentials are included into the Hamiltonian (3), the Floquet theorem says that the eigenstates of this new Hamiltonian can be represented as a superposition of the wavefunctions (4) with shifted energies:

$$\psi_{FL}(x, y, t) = \sum_{n=-\infty}^{\infty} \psi_{\lambda,n}(x, y) e^{-in\omega t} e^{-i\frac{E_\lambda}{\hbar} t}, \quad (7)$$

with

$$\psi_{\lambda,n}(x, y) = C_\lambda \chi_\lambda(y) e^{ik_n x}, \quad (8)$$

$$k_n = \sqrt{\frac{2m^* \omega_0^2 + \omega_c^2}{\hbar^2 \omega_0^2}} \left[E_F + n\hbar\omega - \frac{1}{2} \hbar \sqrt{\omega_0^2 + \omega_c^2} \right]^{1/2} \quad (9)$$

The wavevector (9) applies for the lowest Landau level. The scattering amplitudes are obtained by matching (7) at the boundaries $x = -\frac{L}{2}$ and $x = \frac{L}{2}$. For an electron coming from the left the wavefunctions to be matched are given by

$$\psi_{FL}(x < -\frac{L}{2}) = e^{ik_0 x} + \sum_{n=-\infty}^{\infty} r_n e^{-ik_n x} e^{-in\omega t} \quad (10)$$

$$\psi_{FL}(-\frac{L}{2} < x < \frac{L}{2}) = \sum_{n=-\infty}^{\infty} (A_n e^{ik_n x} + B_n e^{-ik_n x}) \times e^{-in\omega t} \quad (11)$$

$$\psi_{FL}(x > \frac{L}{2}) = \sum_{n=-\infty}^{\infty} t_n e^{ik_n x} e^{-in\omega t}. \quad (12)$$

Similar wavefunctions apply for electrons incident from the right. Here we have omitted the time-dependent factor $e^{-i\frac{E_0}{\hbar}t}$ and transverse wavefunction $\chi_1(y)$, since they are common to all wavefunctions. Following the same procedure as in Appendix A of Ref.¹⁴, we arrive at the result

$$r_n = (A_n - \delta_{n,0})e^{-ik_n L} + B_n \quad (13a)$$

$$t_n = A_n + B_n e^{-ik_n L}, \quad (13b)$$

where A_n and B_n are given by recursion relations (Eqs. (A10)-(A16) in Ref.¹⁴ with k_n given by Eq. (9)). We have solved these equations and calculated the resulting current numerically. Before discussing this result, let us look at the special case of weak pumping, for which an analytic solution can be obtained. Weak pumping is characterized by $\delta V_{AB(AC)} \ll \bar{V}_{AB(AC)}$. Assuming, for simplicity, equal QPCs with $\bar{V}_{AB} = \bar{V}_{AC} \equiv \frac{\hbar^2}{m^*}p$ and $\delta V_{AB} = \delta V_{AC} \equiv \frac{\hbar^2}{m^*}q$, this translates into the requirement $q \ll k_0$. In this case it is easy to show that the scattering probability into the sideband with energy $E_n = E + n\hbar\omega$ is proportional to $\left(\frac{q^2}{k_0^2}\right)^{|n|}$, so that in good approximation only the lowest sideband for $n = \pm 1$ has to be taken into account. We then set $A_{\pm 2} = B_{\pm 2} = 0$ in the recursion relations of Ref.¹⁴ and calculate A_0 , $A_{\pm 1}$, B_0 and $B_{\pm 1}$. For nearly-open QPCs, with $p \ll k_0$, this yields the transmission amplitudes, to lowest order in q/k_0 ,

$$t_{31,0} = 1 + 2i\frac{q^2}{k_0^2} \sin(k_0 L) (e^{i\phi} e^{ik_1 L} + e^{-i\phi} e^{ik_{-1} L}) \quad (14a)$$

$$t_{31,\pm 1} = -i\frac{q}{k_0} \left(e^{-i(k_0 - k_{\pm 1})\frac{L}{2}} + e^{\mp i\phi} e^{i(k_0 - k_{\pm 1})\frac{L}{2}} \right) \quad (14b)$$

$$t_{13,0} = 1 + 2i\frac{q^2}{k_0^2} \sin(k_0 L) (e^{-i\phi} e^{ik_1 L} + e^{i\phi} e^{ik_{-1} L}) \quad (14c)$$

$$t_{13,\pm 1} = -i\frac{q}{k_0} \left(e^{-i(k_0 - k_{\pm 1})\frac{L}{2}} + e^{\pm i\phi} e^{i(k_0 - k_{\pm 1})\frac{L}{2}} \right) \quad (14d)$$

The resulting current is given by

$$\begin{aligned} I_3 &= -I_1 \\ &= -8\frac{e}{h}q^2 \sin \phi \int dE f(E) \frac{1}{k_0^2} \cos(2\tilde{k}_0 L) \sin(\epsilon \tilde{k}_0 L) \quad (15a) \\ &\approx -8\frac{e}{h}\mu \frac{q^2}{k_0^2} \sin \phi \cos(2k_0 L) \sin(\epsilon k_0 L) \text{ for } k_B T \ll \hbar\omega \end{aligned}$$

with

$$\epsilon \equiv \frac{1}{2} \frac{\hbar\omega}{E_F - \frac{1}{2}\hbar\sqrt{\omega_0^2 + \omega_c^2}} \quad \text{and} \quad \tilde{k}_0 = k_0(E_F \rightarrow E)$$

For $\epsilon k_0 L \ll 1$ the current (15b) is directly proportional to the pumping frequency ω . In the derivation of Eq. (15) we have assumed that $\epsilon \ll 1$, which is true for typical system parameters, see Sec. IV. In this

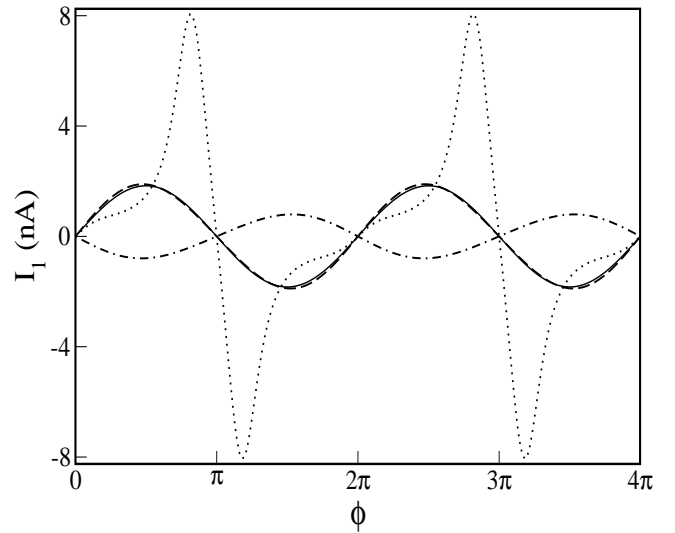


FIG. 2: The current I_1 pumped into contact 1 as a function of the phase difference ϕ . Parameters used are : $B = 7 T$, $m^* = 0.61 \cdot 10^{-31} kg$ (for GaAs), $\omega_c = 1.836 \cdot 10^{13} s^{-1}$, $\omega_0 = 0.08 \omega_c$ ¹⁸, $E_F = 1.716 \cdot 10^{-21} J$ (for $n_e = 3 \cdot 10^{15} m^{-2}$), $L = 300 nm$ ²¹, and $\omega = 10^8 s^{-1}$. The solid line represents the analytical result Eq. (15b), and the other lines represent numerical results for $p/k_0 = 1/10$, $q/k_0 = 1/6$ (dashed line), $p/k_0 = 7/6$, $q/k_0 = 1/6$ (dot-dashed line), $p/k_0 = 1/10$, $q/k_0 = 1$ (dotted line).

case $k_n = k_0 \sqrt{1 + 2n\epsilon} \approx k_0 + k_0 n\epsilon$ for n not too large ($n\epsilon \ll 1$), so certainly in the situation of weak pumping. One may then use this expression of k_n in the exponents and set $k_n \approx k_0$ in the prefactors. The latter is analogous to the Andreev approximation which is often made in calculations involving NS interfaces²⁰.

Fig. 2 shows the pumped current I_1 as a function of the phase difference ϕ at low temperatures in the weak and strong pumping limits. As expected, in the weak pumping limit and for nearly-open QPCs the numerical result (dashed line) agrees very well with the analytical one (solid line). The current is proportional to $\sin \phi$ and we have checked that it displays other typical pumping characteristics such as being linearly proportional to both the frequency ω and the pumping amplitude squared (q^2)²². Also for less open QPCs (dot-dashed line for which the transmission probability of both QPCs $T_{AB} = T_{AC} \approx 0.57$) the pumped current behaves in the same way, the main difference being that it now has a smaller amplitude. For higher pumping strength the current acquires a more complex structure (dotted line). It is not proportional to $\sin \phi$ anymore, although it is still periodic. For the set of parameters used here, the current spreads over ± 40 sidebands upon scattering at each QPC, many more than in the weak pumping regime.

III. HALL AND LONGITUDINAL RESISTANCE

Having found that a current can be pumped across a Hall bar in the absence of a bias voltage, it is interesting to ask what resistance corresponds to this current. In the usual integer quantum Hall effect a current is driven through a Hall bar at low temperatures and gives rise to a resistance parallel to the direction of the current (the longitudinal resistance R_{xx}) and a resistance perpendicular to the direction of the current (the Hall resistance R_H)²³. When measured as a function of the applied magnetic field, the Hall resistance exhibits plateaus at integer multiples of h/e^2 , a new plateau appearing when the number of filled Landau levels changes by one. The explanation for the appearance of the plateaus, on which the resistance does not change, lies in the presence of disorder in the system. This leads to the formation of localized states which in turn lead to the quantization because, roughly speaking, when the Fermi energy moves through an energy band of localized states the number of conduction electrons and hence the Hall resistance does not change. For the same reason, the longitudinal resistance vanishes on the plateaus since the localized electrons cannot dissipate energy by making a transition to a state that is lower in energy. When a new Landau level is occupied (or emptied) and the Hall resistance jumps to the next plateau, the longitudinal resistance exhibits a peak before returning to zero.

How, then, is the behavior of R_H and R_{xx} if the current is not driven through the sample but pumped, as described in the above? Is the Hall resistance then also quantized and does the longitudinal resistance also vanish? Studying the configuration of Fig. 1 we will argue in the following that the answer to the first question is yes and to the second question is no.

Consider again the Hall bar of Fig. 1 in the regime of $\nu = 1$ and assume that the QPC's transmit at most one edge channel during the entire pumping cycle, so the conductance G_{AB} , $G_{AC} \leq \frac{e^2}{h}$. In the absence of scattering at the QPC's all three terminals are at the same chemical potential μ . In order to calculate R_{xx} and R_H we first look at the voltage drop across terminals 1 and 2 (for R_H) and 2 and 3 (for R_{xx}). Let $R_{\alpha\beta} = \sum_n |r_{\alpha\beta}|^2$ and $T_{\alpha\beta} = \sum_n |t_{\alpha\beta}|^2$ denote the reflection and transmission probabilities from contact β to contact α . Analyzing incoming and outgoing currents at zero temperature, the three contacts are then characterized by the chemical potentials²⁴

$$\begin{aligned}\mu_1 &= (R_{12} + T_{13})\mu \\ \mu_2 &= \mu \\ \mu_3 &= (R_{33} + T_{32})\mu.\end{aligned}$$

These lead to the voltage drops

$$\begin{aligned}V_H \equiv V_2 - V_1 &= (1 - R_{12} - T_{13})\frac{\mu}{e} = (T_{32} - T_{13})\frac{\mu}{e} \\ V_{xx} \equiv V_3 - V_2 &= (T_{32} + R_{33} - 1)\frac{\mu}{e} = (T_{32} - T_{13})\frac{\mu}{e}.\end{aligned}$$

Here we have used the conservation laws $T_{13} + R_{33} = 1$ and $R_{12} + T_{32} = 1$. It thus turns out that the parallel and perpendicular voltage drops are the same, $V_H = V_{xx} \equiv V$, and hence that the Hall resistance and longitudinal resistance are equal:

$$R_H = R_{xx} = \frac{V}{I_3} = \frac{h}{e^2}. \quad (16)$$

In the last step of (16) we have used Eq.(2) for the current I_3 at low temperatures $k_B T \ll \mu$. The same result would also be obtained at higher temperatures. Eq. (16) is valid on a plateau, when the Fermi energy lies in a subband of localized states. The reason why R_H is quantized is the same as in the usual IQHE, and due to the presence of impurities. More surprising, at first sight, is the quantization of R_{xx} and it being equal to R_H . When looking more closely at Fig. 1, the reason for this becomes clear and lies in the intrinsic scattering nature of quantum pumping. The presence of scattering, here in the form of the two QPC's, is essential to obtain a pumped current: in the absence of the QPC's no such current would flow. Moreover, even in the presence of the QPC's but if they are wider and transmit more than 1 edge channel, no current would flow: the time-dependent voltages would periodically push the edge channel a bit more inwards, so that the electrons flow along and around the barriers imposed by the voltage leads, and no net current would be pumped into contact 1 or 3. In short, to obtain a pumped current it is required that (part of) the electrons are scattered. As a result, dissipation also occurs in the direction parallel to the current flow and hence R_{xx} never drops to zero. This was also found for the usual IQHE, if the Hall bar contains one or more QPC's¹⁷. At the same time, due to the absence of a bias voltage, the difference between parallel and perpendicular resistance vanishes²⁵. Each outgoing electron from contact 2 or 3 is scattered into either contact 1 or 3. Since the outgoing electrons are all at the same chemical potential and the current is conserved, both V_H and V_{xx} only depend on the difference between the transmission probabilities from 1 to 3 and vice versa.

So far, we have considered filling factor $\nu = 1$ and QPC's with transmission less than unity. What happens at higher filling factors and different transmission of the QPC's? Let $\nu = n$ and assume the QPC's, still taken to be equal, transmit m edge channels (with n and m both integers) plus a fraction T , with $0 \leq T \leq 1$, of the $(m+1)$ th channel. Then two situations can be distinguished:

- 1) $n \leq m \rightarrow$ no pumping takes place, all edge channels are transmitted without scattering.
- 2) $n > m \rightarrow$ The $(m+1)$ th edge channel gives rise to a pumped current and corresponding

$$\text{resistances } R_H = R_{xx} = \frac{h}{ne^2}.$$

As a function of decreasing magnetic field, or equivalently increasing filling factor ν , the Hall resistance thus rises

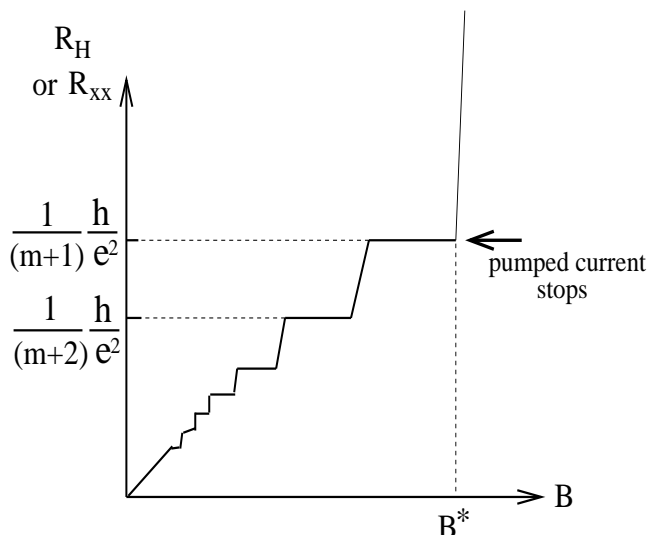


FIG. 3: Schematic picture of the Hall resistance R_H and longitudinal resistance R_{xx} as a function of the applied magnetic field B . At B^* the $(m+1)$ th Landau level becomes occupied, with m the highest Landau level which is still fully transmitted by the QPC's.

from 0 to the value $\frac{h}{(m+1)e^2}$ as soon as the $(m+1)$ th Landau level becomes occupied at magnetic field B^* . This is depicted in Fig. 3. For higher filling factors the resistance decreases in steps, just as in the usual IQHE. Similar arguments apply if the transmission probabilities of the two QPC's are not equal.

IV. DISCUSSION AND CONCLUSIONS

In this final section, let us look at realistic experimental parameters in order to quantify our results. Typical Hall

bars are several 100 μm long and about 100 μm wide¹⁷. Present-day experimental techniques allow for separation of the gates by 200-300 nm²¹, so that the QPC gates can be placed sufficiently far away from the other contacts 1-3 that the applied time-varying voltages do not affect the voltage measurements there. For the parameters used in Fig. 2 (see the caption) and temperatures $T \sim 10$ mK the conditions $k_B T \ll \mu$ and $\epsilon \ll 1$ are fulfilled and a pumped current on the order of 1-10 nA would be generated, well within reach of observation. Our model does not take dephasing effects into account. These are detrimental to quantum pumping, but were found to be small³ at temperatures below 100 mK.

In conclusion, we have found that a dc current can be pumped across a Hall bar containing two QPC's without applying a bias voltage. Just like a current that is driven through the sample, this pumped current gives rise to a Hall and longitudinal resistance. In sharp contrast with the usual IQHE, however, the longitudinal resistance equals the Hall resistance and both exhibit plateaus as a function of the applied magnetic field. A cut-off occurs when the filling factor falls below the number of Landau levels transmitted through the QPC's. Measurement of R_H and/or R_{xx} as a function of the magnetic field can thus be used to deduce ν and the transmission of the QPC's. Also the sharp change in resistance at B^* may be useful, e.g. as a magnetic switch. We hope that these curious properties of quantum pumping in high magnetic fields will find experimental confirmation.

Stimulating discussions with M. Heiblum and Y. Levinson are gratefully acknowledged. This work has been supported by the Stichting voor Fundamenteel Onderzoek der Materie (FOM), and by the EU's Human Potential Research Network under contract No. HPRN-CT-2002-00309 ("QUACS").

-
- ¹ See e.g. B. Spivak, F. Zhou, and M.T. Beal Monod, Phys. Rev. B **51**, 13226 (1995); I.L. Aleiner and A.V. Andreev, Phys. Rev. Lett. **81**, 1286 (1998); T.A. Shutenko, I.L. Aleiner, and B.L. Altshuler, Phys. Rev. B **61**, 10366 (2000); J.E. Avron, A. Elgart, G. M. Graf, and L. Sadun, Phys. Rev. B **62**, 10618 (2000); A. Andreev and A. Kamenev, Phys. Rev. Lett. **85**, 1294 (2000); Y. Makhlin and A.D. Mirlin, Phys. Rev. Lett. **87**, 276803 (2001); M.G. Vavilov, V. Ambegaokar, and I.L. Aleiner, Phys. Rev. B **63**, 195313 (2001); O. Entin-Wohlman, A. Aharony, and Y. Levinson, Phys. Rev. B **65**, 195411 (2002);
² P.W. Brouwer, Phys. Rev. B **58**, R10135 (1998).
³ M. Switkes, C.M. Marcus, K. Campman, and A.D. Gosard, Science **283**, 1905 (1999).
⁴ D.J. Thouless, Phys. Rev. B **27**, 6083 (1983).
⁵ L.P. Kouwenhoven, A.T. Johnson, N.C. van der Vaart, C.J.P.M. Harmans, and C.T. Foxon, Phys. Rev. Lett. **67**, 1626 (1991); H. Pothier, P. Lafarge, C. Urbina, D. Esteve, and M.H. Devoret, Europhys. Lett. **17**, 249 (1992); S.H.

- Simon, Phys. Rev. B **61**, R16327 (2000).
⁶ See e.g. Y. Levinson, O. Entin-Wohlman, and P. Wölfle, Physica A **302**, 335 (2001); Y. Wei, J. Wang, H. Guo, and C. Roland, Phys. Rev. B **64**, 115321 (2001); J.N.H.J. Cremers and P.W. Brouwer, Phys. Rev. B **65**, 115333 (2002); M. Blaauboer, Phys. Rev. B **65**, 235318 (2002); and Refs.^{1,2,3}.
⁷ P. Sharma and C. Chamon, Phys. Rev. Lett. **87**, 096401 (2001); E.R. Mucciolo, C. Chamon, and C.M. Marcus, Phys. Rev. Lett. **89**, 146802 (2002); S.K. Watson, R.M. Potok, C.M. Marcus, and V. Umansky, cond-mat/0302492; P. Sharma and P.W. Brouwer, cond-mat/0306001.
⁸ For a review on electron transport through quantum dots see L.P. Kouwenhoven *et al.*, in *Proceedings of the Advanced Study Institute on Mesoscopic Electron Transport*, L.P. Kouwenhoven, G. Schön, L.L. Sohn, Eds. (Kluwer, Dordrecht, 1997).
⁹ M. Blaauboer, cond-mat/0307166 (preprint).
¹⁰ C.W.J. Beenakker and H. van Houten, Solid State Physics

- 44**, 1 (1991).
- ¹¹ O. Entin-Wohlman, Y. Levinson and P. Wölfle, Phys. Rev. B **64**, 195308 (2001).
 - ¹² The factor of 2 in front of the cosines is introduced for convenience.
 - ¹³ J.H. Shirley, Phys. Rev. **138 B**, 979 (1965); M. Wagner, Phys. Rev. B **49**, 16544 (1994); W. Li and L.E. Reichl, Phys. Rev. B **60**, 15732 (1999).
 - ¹⁴ M. Moskalets and M. Büttiker, Phys. Rev. B **66**, 205320 (2002).
 - ¹⁵ S.-L. Zhu and Z.D. Wang, Phys. Rev. B **65**, 155313 (2002); S.W. Kim, Phys. Rev. B **66**, 235304 (2002).
 - ¹⁶ If spin effects are important, additional terms have to be included in the Hamiltonian (3), such as the Zeeman term $\frac{1}{2}g^*\mu_B B\sigma$ [with g^* the effective g-factor, μ_B the Bohr magneton and $\sigma = 1(-1)$ for electrons with spin up (down)] and, for example, a hyperfine or spin-orbit interaction term.
 - ¹⁷ *Introduction to the Theory of the Integer Quantum Hall Effect*, M. Janssen, O. Viehweger, U. Fastenrath and J. Hajdu, (VCH, Weinheim, 1994); *Electronic Transport in Mesoscopic Systems*, S. Datta (Cambridge University Press, Cambridge, 1995).
 - ¹⁸ S.B. Haley and H.J. Fink, Phys. Rev. B **60**, 8225 (1999).
 - ¹⁹ R.B. Laughlin, Rev. Mod. Phys. **71**, 863 (1998).
 - ²⁰ A.F. Andreev, Zh. Éksp. Teor. Fiz. **46**, 1823 (1964) [Sov. Phys. JETP **19**, 1228 (1964)], **51**, 1510 (1966) [**24**, 1019 (1967)]; See also the discussion in M. Blaauboer, R.T.W. Koperdraad, A. Lodder, and D. Lenstra, Phys. Rev. B **54**, 4283 (1996).
 - ²¹ J.M. Elzerman, R. Hanson, J.S. Greidanus, L.H. Willems van Beveren, S. De Franceschi, L.M.K. Vandersypen, S. Tarucha, and L.P. Kouwenhoven, Phys. Rev. B **67**, 161308(R), 2003.
 - ²² In contrast to quantum pumping in quantum dots, however, the direction of the pumped current in high magnetic fields, such as quantum Hall systems, is fully determined.
 - ²³ For an introduction into the quantum Hall effects see B. Halperin, Scientific American **254**, p.52 (1986) and Ref.¹⁷.
 - ²⁴ M. Büttiker, IBM J. Res. Dev. **32**, 317 (1988); see also S. Datta in Ref.¹⁷.
 - ²⁵ We emphasize that it is thus the fact that current is pumped, and not the details of the geometry, that causes R_H and R_{xx} to be equal.